Chapter 23

Advection schemes

23.1 Test case *cones*

23.1.1 Description of the problem and model setup

The ***cones*** problem is a well known problem for the testing of advection schemes (e.g. Takacs (1985); Ruddick (1995)). A squared-shaped basin is considered bounded by solid walls. The width of the basin is taken as 40 m and the mesh size of the grid is 1 m. A current field is imposed in the form of a solid body rotation with angular velocity Ω around the point (x_0,y_0) located near the centre of the basin

$$u = -\Omega(y - y_0)\ ,\ v = \Omega(x - x_0)\ ,\ w = 0 \tag{23.1}$$

where (x,y) are the horizontal Cartesian coordinates, (u,v) the horizontal components of the current, w the vertical velocity, $\Omega = 1/1200\ \mathrm{s}^{-1}$ and (x_0,y_0) = (19.5,19.5). An initial contaminant distribution, represented in the setup by a salinity field, has a cone shaped form with radius R and centered at (x_c,y_c):

$$C = \max\left[1 - \frac{\sqrt{(x - x_c)^2 + (y - y_c)^2}}{R}, 0\right] \tag{23.2}$$

where $R = 5$, (x_c,y_c) = (10.5,20.5) and C is the contaminant concentration[1] in arbitrary units. The initial current and contaminant field distributions are plotted in Figure 23.1. The program only needs to solve one transport equation. This takes the following simple form in the absence of diffusion, vertical currents, surface elevation and variations in bottom depth

[1]Since there is no contaminant module implemented in the current version, the contaminant distribution is represented here by salinity.

$$\frac{\partial C}{\partial t} + \frac{\partial}{\partial x}(Cu) + \frac{\partial}{\partial y}(Cv) = 0 \tag{23.3}$$

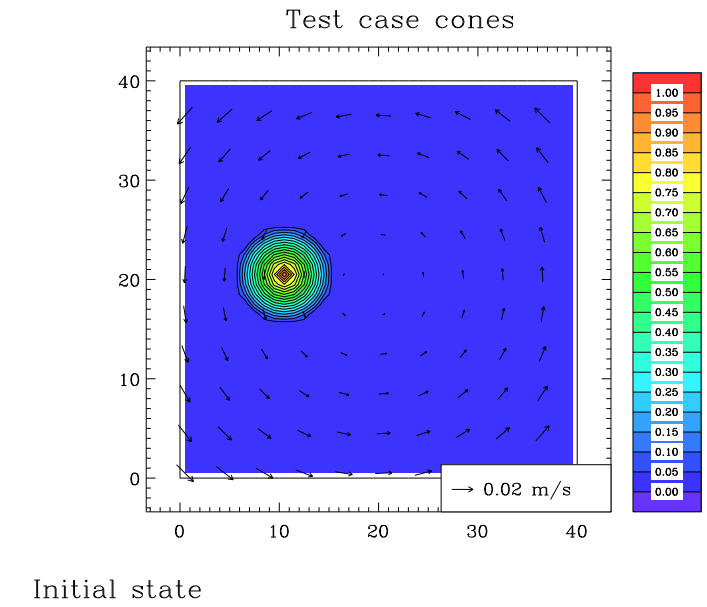

Figure 23.1: The initial configuration of the ***cones*** test case.

23.1.2 Experiments and output parameters

The ***cones*** test intercompares the four scalar advection schemes implemented in the program. The following experiments have been set up:

A **:** upwind scheme

B **:** Lax-Wendroff scheme

C **:** TVD scheme using the superbee limiting function

D **:** TVD scheme using the monotonic limiting function

In each experiment the program is run for two rotation periods. The contaminant distributions at the end of the simulation are given in Figures 23.2 for the four schemes. Figures 23.3 display the surface distributions after two periods of revolution along two transects through the cone centre parallel to respectively the X- and Y-axis.

A series of parameters are defined in the program and written to the *.tst* output files at $t = 0.5T$, T, $1.5T$, $2T$ where T is the rotation period.

xmin The cone radius measured in the negative X-direction (m). This is taken as the distance between the cone centre and the point to the left where C becomes less than 0.01 along a line parallel to the X-axis[2].

xplus The cone radius measured in the positive X-direction (m). This is taken as the distance between the cone centre and the point to the right where C becomes less than 0.01 along a line parallel to the X-axis[2].

ymin The cone radius measured in the negative Y-direction (m). This is taken as the distance between the cone centre and the point below where C becomes less than 0.01 along a line parallel to the Y-axis[2].

yplus The cone radius measured in the positive Y-direction (m). This is taken as the distance between the cone centre and the point above where C becomes less than 0.01 along a line parallel to the Y-axis[2].

cmin Minimum value of the concentration over the entire domain.

cmax Maximum value of the concentration over the entire domain.

Exact values are 5 for the four radii, 0 for cmin and 1 for cmax.

23.1.3 Results

- It is clear that scheme ***C*** which is also the default scheme of the program, gives the best performance both in preserving the original shape as in maintaining the gradient of the contaminant concentration.

- Scheme ***D*** produces a more diffusive and asymmetric distribution and less sharp gradients.

- The upwind scheme ***A*** is only first order accurate and therefore highly diffusive. This is clearly observed in Figure 23.2a where the original distribution has been smeared out over the entire basin.

- Although scheme ***B*** can preserve sharp gradients, the original shape is highly distorted. A further problem is the non-preservation of extremal values yielding even negative concentrations.

[2]If the radius is larger than the distance of the cone centre to the corresponding basin boundary, its value is set to -999.9.

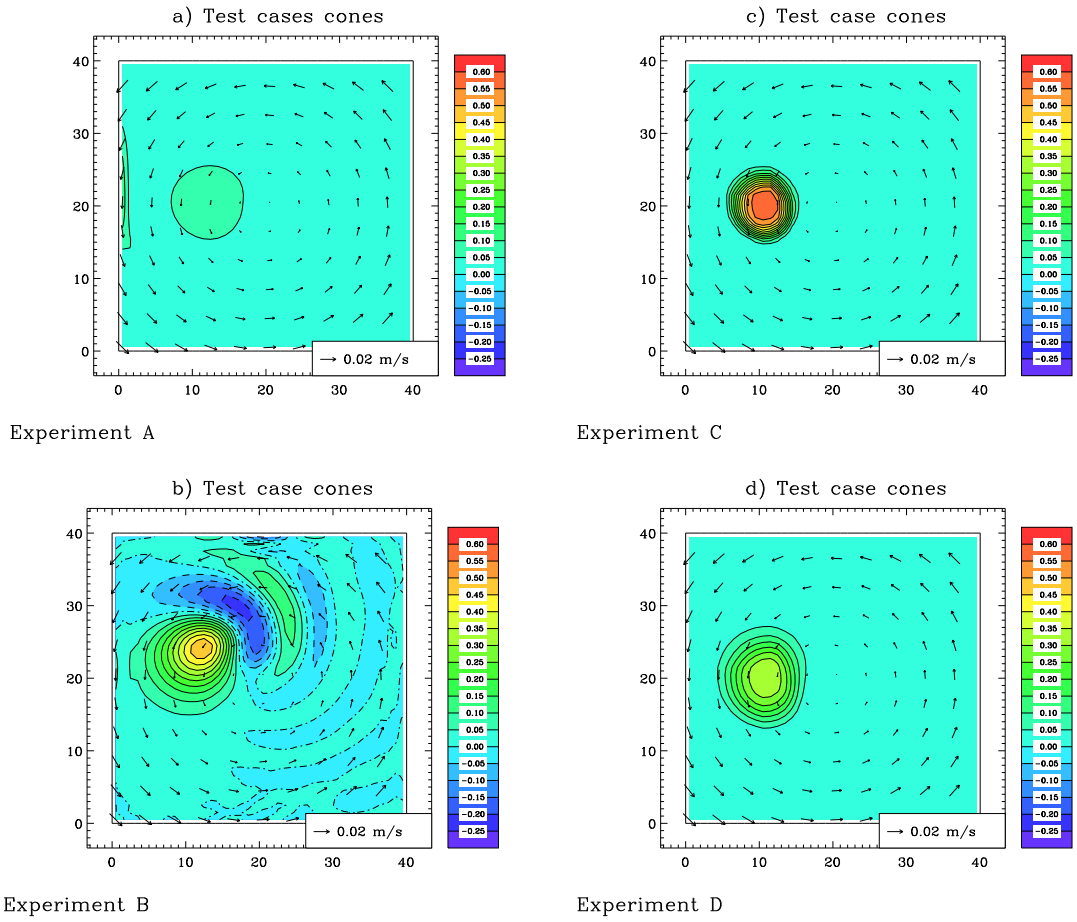

Figure 23.2: Test case ***cones***. Surface concentrations after two periods of revolution for scheme ***A*** (a), ***B*** (b), ***C*** (c), ***D*** (d).

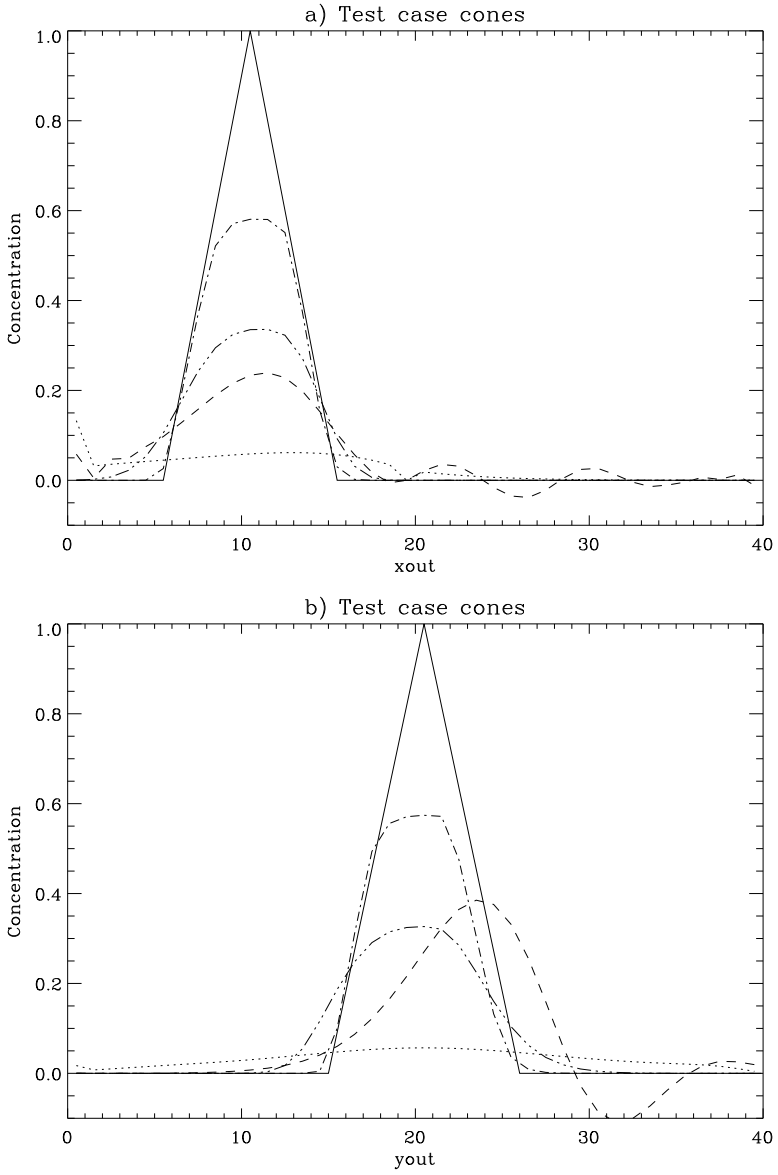

Figure 23.3: Test case ***cones***. Surface concentrations at the end of the simulation along a transect through the cone centre parallel to the X-axis (a) and the Y-axis (b) for the exact case (solid) schemes ***A*** (dots), ***B*** (dashes), ***C*** (dash-dots) and ***D*** (dash plus 3 dots).

23.2 Test case *front*

23.2.1 Description of the problem and model setup

This test case has been designed to verify the horizontal schemes for the advection of scalar quantities. The initial configuration consists of a non-rotating channel with open boundaries at the two ends. The water depth is determined by a piecewise linear profile of the form

$$\begin{array}{lll} H = 50 & \text{for} & 0 < x < 25 \\ H = 150 - 4x & \text{for} & 25 \leq x \leq 30 \\ H = 30 & \text{for} & x > 30 \end{array} \tag{23.4}$$

where H is the water depth in m and x_1 the along-channel distance in km. An initial two-layer distribution is specified by

$$\begin{array}{lll} C = 2 & \text{if} & z_s < 20\ ,\ 0 < x < 25 \\ C = 1 & \text{if} & x \geq 25 \\ C = 0 & \text{if} & z_s \geq 20\ ,\ 0 < x < 25 \end{array} \tag{23.5}$$

where z_s is the distance to the surface in m and C the contaminant concentration in arbitrary units. During the simulation the lateral and horizontal front are advected by an imposed tidal current with a semi-diurnal period:

$$u = u_a(x, z_s)\cos(2\pi t/T) \tag{23.6}$$

where $T = 12$ h. The amplitude u_a in m/s is prescribed by

$$\begin{array}{lll} u_a = 2 & \text{if} & z_s + \Delta z/2 < 30 \\ u_a = 0 & \text{if} & z_s - \Delta z/2 > 30 \\ u_a = 2(30 - z_s + \Delta z/2)/\Delta z & \text{otherwise} & \end{array} \tag{23.7}$$

where Δz is the vertical grid spacing. The model uses a σ-coordinate system with 20 vertical levels so that the vertical grid spacing Δz, following (23.4) varies horizontally 2.5 m in the deepest part to 1.5 m in the shallowest part of the domain.

The program only solves two equations: the transport equation for the contaminant concentration without diffusion and the continuity equation for the vertical velocity. The latter is non-zero only along the slope where the prescribed velocity field has a non-zero horizontal gradient. The channel length is set to 50 km. All cross-channel variations are neglected.

23.2.2 Experiments and output parameters

In analogy with the ***cones*** test case the ***front*** case is an idealised problem enabling to intercompare the different advection schemes implemented in the program using simple forcing and initial conditions. The same four tests have been set up:

A **:** upwind scheme

B **:** Lax-Wendroff scheme

C **:** TVD scheme using the superbee limiting function

D **:** TVD scheme using the monotonic limiting function

The simulations are performed for 36 hours, i.e. 3 semi-diurnal tidal cycles. The contaminant distributions and current field are displayed in Figures 23.4 at the initial time and at 3 h intervals during the last cycle for scheme ***C*** which is also the default scheme of the program. The distributions after 27 hours are compared for the four experiments in Figures 23.5. The concentrations at 5 m below the surface and a vertical profile at 30 km from the left boundary are shown in Figures 23.6 after 27 hours of simulation.

The following output test parameters are defined

gradh The maximum horizontal gradient (km^{-1}) along an horizontal transect taken at 5 m depth below the surface.

gradv The maximum vertical gradient (m^{-1}) along a moving vertical transect taken at the left edge of the lateral front.

hleng The width of the lateral front measured in km at 5 m below the surface. This is defined as the horizontal width of the area where the horizontal gradient is larger than 0.01 km^{-1}.

cmin Minimum concentration along the moving vertical transect.

cmax Maximum concentration along the moving vertical transect.

Values for the exact case are 1 (gradh, hleng), 0.8 (gradv), 0 (cmin), 2 (cmax).

23.2.3 Results

- After an initial broadening due to numerical diffusion, the shape of the fronts remains unchanged after a tidal cycle as can be seen by comparing Figures 23.4b and f.

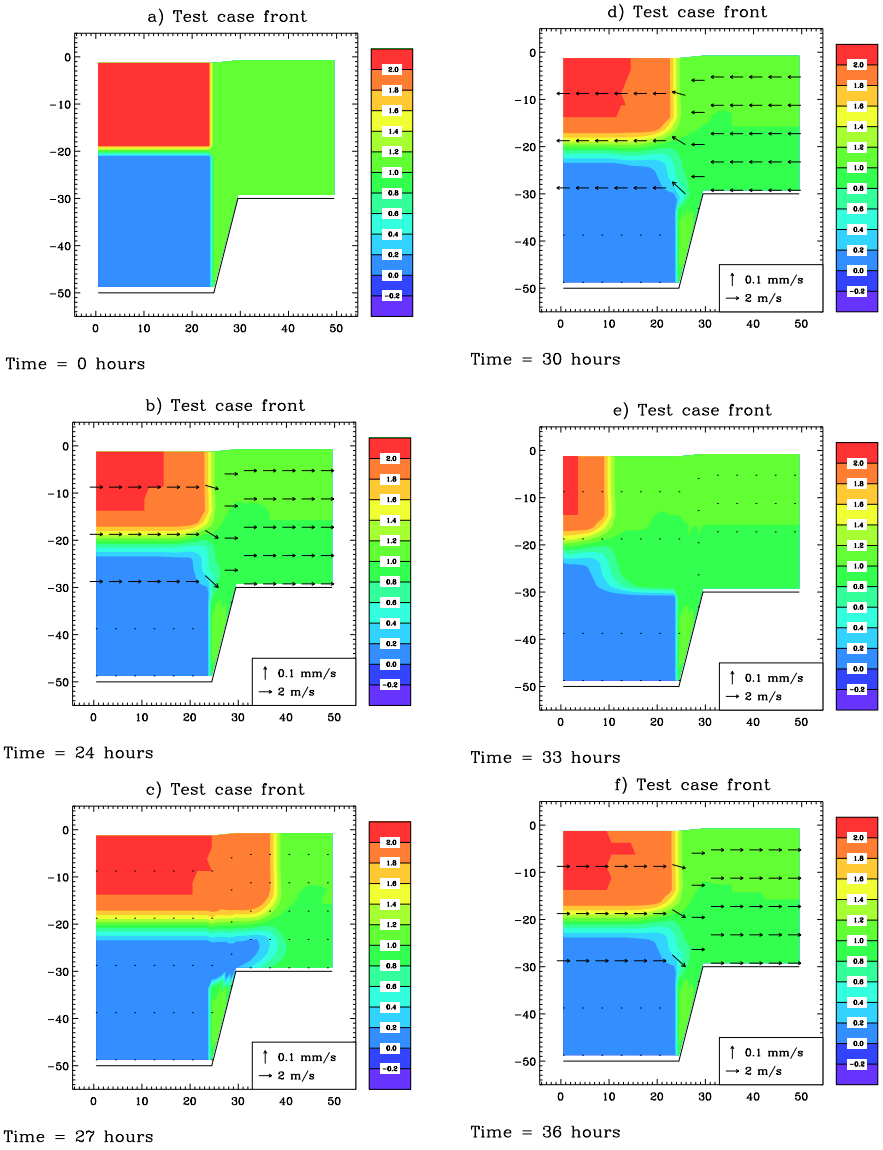

Figure 23.4: Test case ***front***. Contaminant distribution and current field for experiment ***C*** at $t = 0$ h (a), $t = 24$ h (b), $t = 27$ h (c), $t = 30$ h (d), $t = 33$ h (e), $t = 36$ h (f).

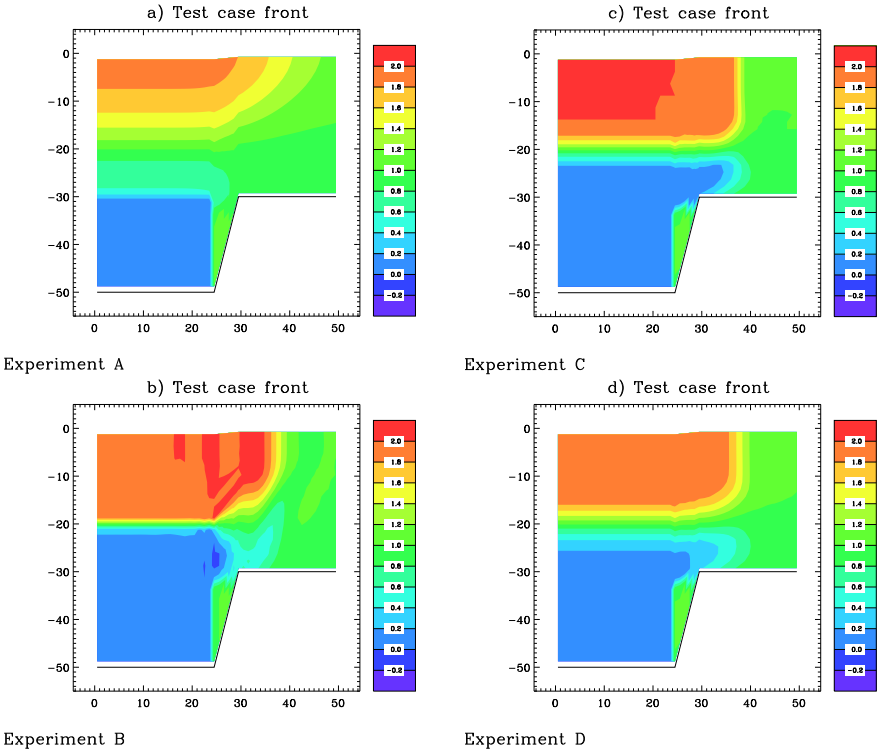

Figure 23.5: Test case ***front***. Contaminant concentration after 27 hours for scheme ***A*** (a), ***B*** (b), ***C*** (c), ***D*** (d). Contour lines are at 0.2 intervals.

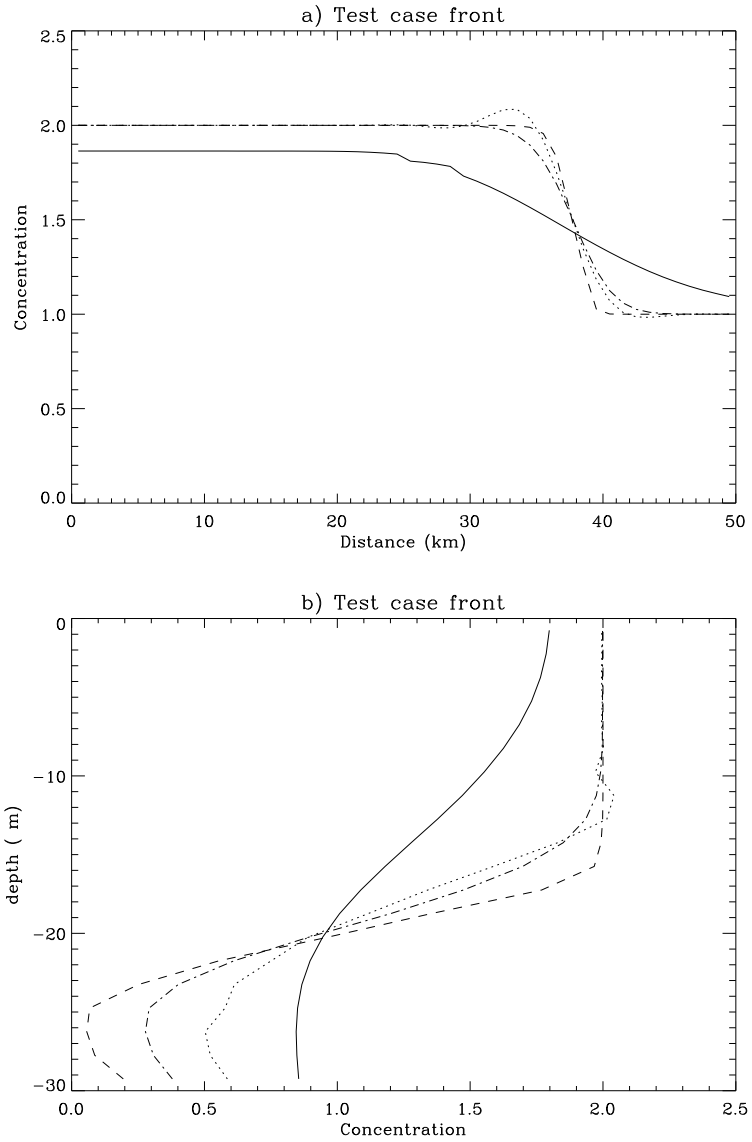

Figure 23.6: Test case ***front***. Contaminant concentration after 27 hours for scheme ***A*** (solid), ***B*** (dots), ***C*** (dashes) and ***D*** (dash-dots): horizontal profile at 5 m below the surface (a), vertical profile at 30 km from the left boundary (b).

- Comparing the test results for the different experiments shows that the default scheme ***C*** not only produces the sharpest (lateral) front (parameter gradh) but also the smallest frontal width (parameter hleng).

- The importance of the type of advection scheme for the simulation of frontal systems can be further observed in Figures 23.5. The upwind scheme, which is only first order accurate, is the most diffusive. Schemes C and D are similar although the latter is somewhat more diffusive. A sharp horizontal front is also produced by the second order Lax-Wendroff scheme. A clear disadvantage is that this scheme does not preserve monotonicity resulting in spurious over- and undershooting along the lateral front. The same features can also be inferred from Figures 23.6a–b. The results are clearly in agreement with the previous ***cones*** test.

23.3 Test case *seich*

23.3.1 Description of the problem and model setup

The previous two problems served to test the advection schemes for scalar quantities. They are idealistic in the sense that the velocity is not updated by the program but prescribed externally. A more realistic test case is the ***seich*** problem where a two-dimensional circulation along a vertical plane is generated through an horizontal pressure gradient. The main aim is to verify the advection schemes for momentum and scalars and to test the circulation module.

A non-rotating channel, 30 km long, with a uniform depth of 20 m is considered bounded by a solid lateral wall at the two ends. All cross-channel variations are neglected. The initial surface elevation is set to zero. A salinity stratification is specified initially in a two-layer form with a fresh water value of $S_1 = 25$ PSU in the upper and a sea water value of $S_2 = 35$ PSU in the lower layer. The interface is located at a depth of 7.5 m in the left and 12.5 m in the right portion of the channel. In the middle of the channel the interface decreases with a uniform slope of 0.0025 m^{-1}. The upper layer density is related to salinity via a linear equation of state of the form

$$\rho_1 = \rho_2(1 + \beta_S(S_1 - S_2)) \tag{23.8}$$

where ρ_1, ρ_2 are the densities in the upper, respectively lower layer and β_S is the uniform salinity expansion coefficient. The initial state is shown in Figure 23.7. The resulting horizontal (baroclinic) pressure gradient creates, in

the absence of vertical and horizontal diffusion, an horizontal motion through a balance with the inertial force in the momentum equation and a vertical current via the continuity equation. The program solves all momentum (2-D and 3-D) equations, the equation of continuity (2-D and 3-D) and the transport equation for salinity. Spatial resolution is 500 m in the horizontal and 1 m in the vertical.

23.3.2 Analytical solution

The problem can be solved analytically provided that all non-linear terms are neglected in the momentum and continuity equation. This assumption is validated by the numerical solutions presented below. The general solution consists of a combination of four modes: two internal (baroclinic) modes propagating in opposite along-channel directions with a wave speed $c_i = 2.2$ km/h and two external (barotropic) modes propagating in the same opposite directions with a larger speed $c_e = 50$ km/h. Since the initial surface elevation is set to zero, the latter modes only have a negligible impact. As a consequence the slope front in the middle of the channel splits in two equal parts. The upper (lower) part moves with speed $-c_i$ to the left (right). Vertical motions are generated above and below the slope front which are downwards directed along the leftward moving front and upward along the rightward moving front. The circulation is closed between the two fronts by an horizontal current towards the left in the upper and towards the right in the lower layer. This evolution is illustrated in Figures 23.8a–c showing the circulation and the front after 1, 3, and 6 hours. The frontal system reaches the boundaries of the domain after nearly 7 hours.

23.3.3 Experiments and output parameters

To test firstly the influence of the advection of momentum and secondly the type of advection scheme the following four experiments have been defined:

A **:** advection of momentum switched off, TVD scheme for salinity

B **:** upwind scheme for momentum and salinity

C **:** upwind scheme for momentum, TVD scheme for salinity

D **:** TVD scheme for momentum, upwind scheme for salinity

E **:** TVD scheme for momentum and salinity

Experiment ***C*** uses the default scheme implemented in the program. The simulations are performed for a period of 7 hours. The results obtained with scheme ***C*** are compared with the analytical solution in Figures 23.8a–f. The five experiments are compared in Figures 23.9 showing the distributions after 4 hours.

The following output parameters are defined

hleft The distance (km) of the leftward moving front with respect to the centre of the channel. The position of the front is taken at the location where the vertical current in the upper layer attains its largest negative value.

hright The distance (km) of the rightward moving front with respect to the centre of the channel. The position of the front is taken at the location where the vertical current in the lower layer attains its largest positive value.

v2up The value of the horizontal current (m/s) in the upper layer averaged between the two fronts.

v2lo The value of the horizontal current (m/s) in the lower layer averaged between the two fronts.

wmaxup Maximum value of the vertical current (mm/s) in the upper layer.

wmaxlo Maximum value of the vertical current (mm/s) in the lower layer.

wminup Minimum value of the vertical current (mm/s) in the upper layer.

wminlo Minimum value of the vertical current (mm/s) in the lower layer.

sdev The relative difference between the volume averaged salinity and its initial value, defined by

$$\mathsf{sdev} = 10^7(\langle S(t)\rangle - \langle S(0)\rangle)/\langle S(0)\rangle \tag{23.9}$$

where a $\langle\ \rangle$ denotes the averaged value over the whole width and depth of the channel. Since the salinity fluxes are zero at the surface, the bottom and along the solid side walls, the exact value of SDEV is zero. Since the numerical schemes for the advection of salinity are conservative, non-zero values are only produced by rounding errors. This parameter is therefore useful to test the machine accuracy.

In the definition of the above parameters the upper and lower layer are conveniently taken at respectively 5.5 below the surface and 4.5 above the bottom. Values for the analytical solution are given in Table 23.1.

Table 23.1: Output values for the analytical solution of test case ***seich***.

time (h)	1	2	3	4	5	6
hleft	2.750	5.250	7.250	9.750	11.75	13.75
hright	2.750	5.250	7.250	9.750	11.75	13.75
v2up	-0.1188	-0.1273	-0.1358	-0.1355	-0.1392	-0.1417
v2lo	0.1316	0.1401	0.1486	0.1483	0.1520	0.1545
wmaxup	0.4180	0.4180	0.4180	0.4179	0.4180	0.4180
wmaxlo	0.3432	0.3433	0.3432	0.3433	0.3433	0.3432
wminup	-0.4185	-0.4185	-0.4185	-0.4186	-0.4185	-0.4185
wminlo	-0.3431	-0.3431	-0.3431	-0.3431	-0.3431	-0.3431
sdev	0	0	0	0	0	0

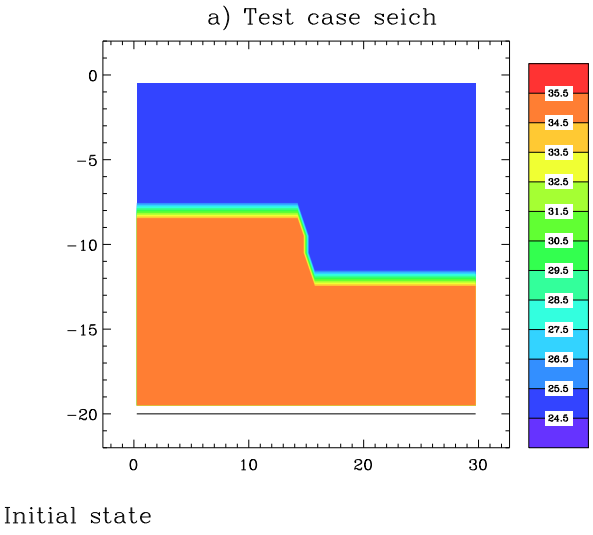

Figure 23.7: The initial configuration of the ***seich*** test case.

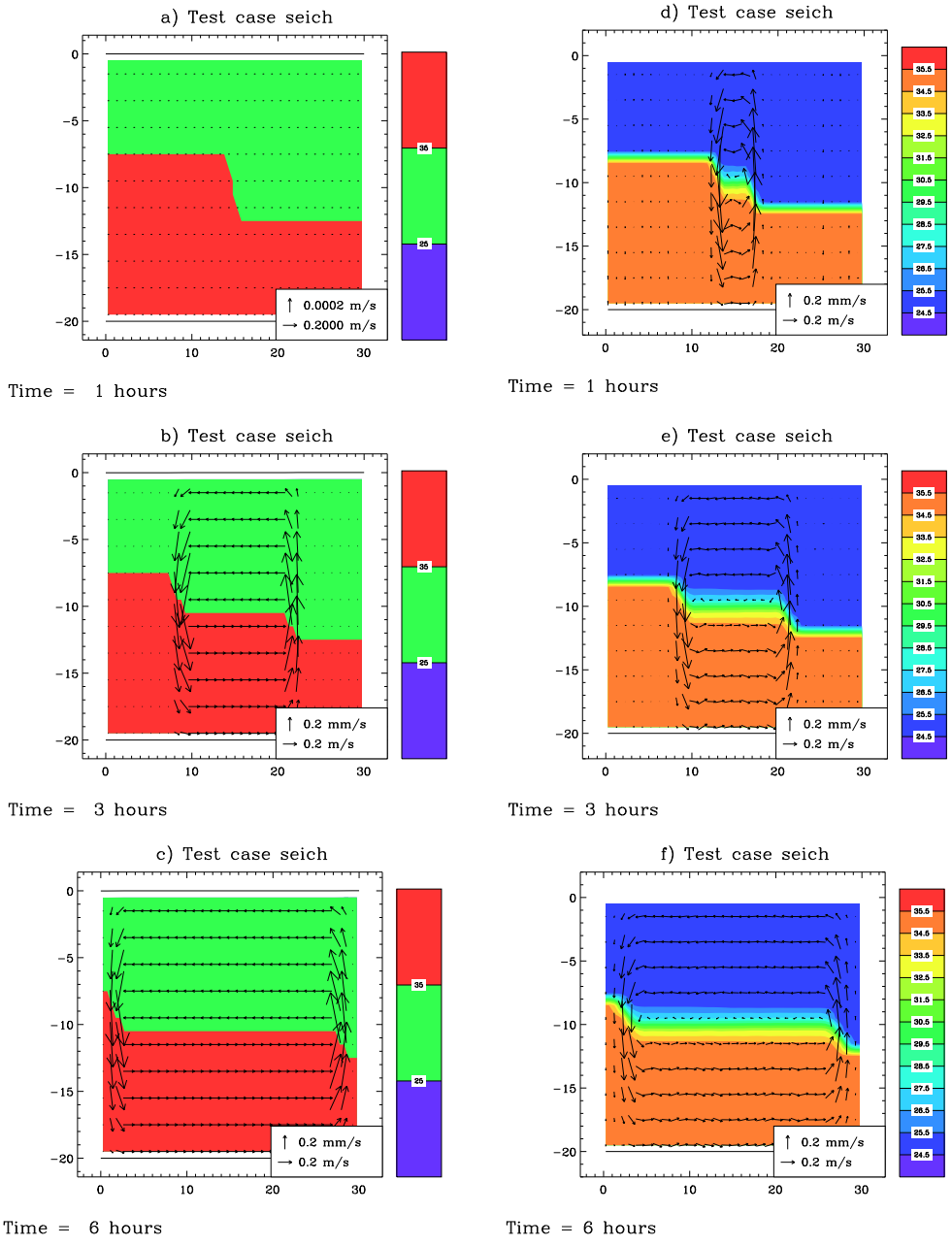

Figure 23.8: Evolution of the current field, salinity and the frontal system for the ***seich*** test case after 1, 3, and 6 hours according to the analytical theory (a, b, c) and experiment ***C*** (d, e, f).

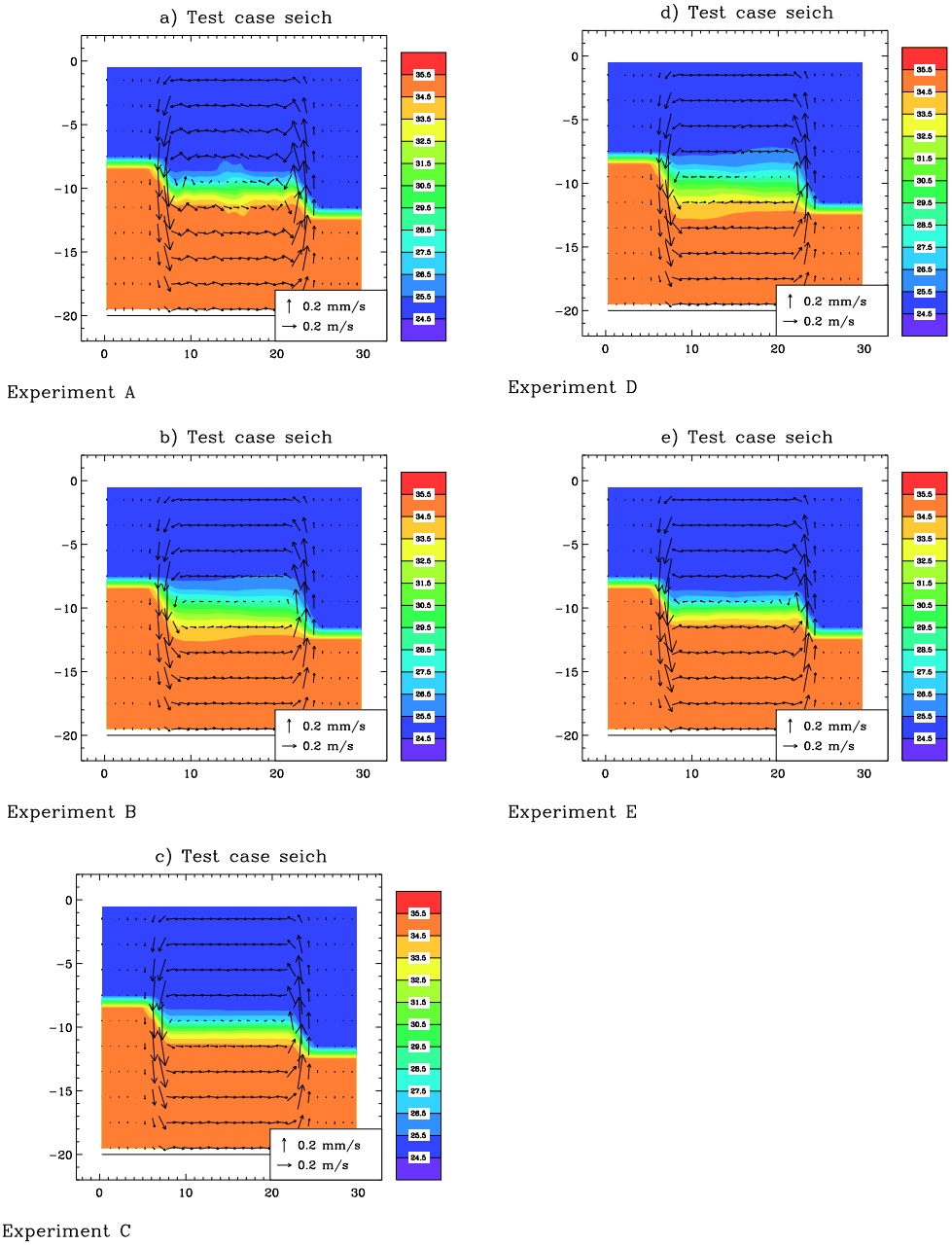

Figure 23.9: Current field and salinity distribution for the ***seich*** test case after 4 hours using scheme ***A*** (a), ***B*** (b), ***C*** (c), ***D*** (d) and ***E*** (e).

23.3.4 Results

- It should be remarked first that contrary to the numerical setup the analytical derivation assumes that the channel has open ends allowing the perturbation to propagate towards infinity. This explains the (barely visible) small perturbation in the current field outside the fronts caused by the barotropic mode which already attains the edges of the channel after 17 min and bounces off the solid walls. The model appears in good agreement with the analytical theory. A notable difference is the initial occurrence of spurious oscillations of the current field gradually attenuating in time. Note also that the interface which separates the upper and lower layer between the two fronts is spread over 3–4 m (or grid cells). The interface thickness remains however uniform in time.

- The numerical oscillations of the current field are more clearly observed in the case of scheme ***A*** which does not advect momentum, whereas they are almost absent in the other runs due to numerical diffusion by the advection scheme. Note also the larger thickness of the interface when the salinity is advected by the upwind scheme (experiments ***B*** and ***D***).

- Comparing the values of the parameters hleft and hright for the analytical case and the four experiments it is seen that the fronts advance more slowly to the left and the right in the model results. This indicates that the internal wave speed c_i is somewhat underestimated by the model. Best agreement is found for experiments ***C*** and ***E*** using the TVD scheme for salinity.

- The magnitude of the horizontal current is underestimated by the model in the upper and lower layers. However, the horizontal kinetic energy has the tendency to increase in all cases. This occurs at the expense of potential energy which decreases while the fronts are moving.

- The vertical velocity is non-zero only above and below the points where the interface has a non-zero gradient. The maximum and minimum values within the upper and lower layer are time-independent in the analytical solution which is not the case in the model results where the magnitude of the vertical current decreases with time both in the upper and the lower layer. This may be due to numerical diffusion. Best agreement is for experiment ***E***.

- All scalar advection schemes are discretised in a conservative form within the program. This means that sdev should be zero in the absence

of rounding errors. The magnitude of this parameter has a maximum value mostly below 4×10^{-7} which may considered as sufficiently accurate.

23.4 Test case *fredy*

23.4.1 Description of the problem and model setup

The test case ***fredy*** is a 3-D problem intended to compare the advection schemes of momentum and scalars and was used previously in the MAST-NOMADS project (Proctor, 1997) as an intercomparison study for shelf sea models. The results of the exercise are described in Tartinville *et al.* (1998). The initial setup of the problem is based upon an earlier numerical study of James (1996). An analogous series of laboratory experiments has been conducted by Griffiths & Linden (1981) whereby a bottomless cylinder of fresh water is immersed into a rotating tank containing a fluid of higher density. After removal of the cylinder the fresh water spreads radially outwards until a geostrophic quasi-equilibrium state is reached. During the next stage non-axisymmetric instabilities develop in the form of growing vortices at the edge of the cylindrical area. The number of vortices is determined by the growth rate of the most unstable mode which depends on the initial parameters of the experiment. The laboratory results bear resemblance to those obtained by Madec *et al.* (1991) who investigated numerically the process of deep water formation in the Mediterranean Sea and found similar eddy-like structures.

The setup used in test case ***fredy*** is almost the same as in Tartinville *et al.* (1998). A 20 m deep squared basin is considered. The domain is closed by four solid boundaries and the basin has a width of 60 km to minimise the influence of the side walls. The grid resolution is 1 km in the horizontal and 1 m in the vertical[3]. The initial salinity distribution in PSU, shown in Figures 23.10 is given by

$$\begin{aligned} S &= 1.1(D/3)^8 + 33.75 \quad \text{if} \quad D \leq 3 \quad \text{and} \quad d \leq 10 \\ &= 34.85 \quad \text{otherwise} \end{aligned} \tag{23.10}$$

where D is the distance in km to the axis of the cylinder, located at (29.5,29.5) in Figure 23.10 (left) and d denotes the depth in m. The density is determined with the aid of the equation of state

$$\rho = \rho_0(1 + \beta_S(S - S_0)) \tag{23.11}$$

[3]For convenience, the outer 15 km of the basin are not displayed in Figures 23.10–23.13.

The simulated area is located at $52^0 3'$N with a corresponding Coriolis frequency of 1.15×10^{-4} s^{-1}.

The initial current and surface elevation are set to zero. The problem is further simplified by neglecting all diffusion terms and setting the surface and bottom stress equal to zero. The simulation is performed for a period of 6 days. The program solves the following equations: the 2-D and 3-D momentum and continuity equations, and the salinity equation.

23.4.2 Experiments and output parameters

The results, presented in Tartinville *et al.* (1998), clearly show that the type of advection scheme, used for momentum and salinity, has an important influence on the development and structure of the baroclinic eddies. Only the upwind and TVD scheme with the superbee limiter are considered in the present study. The following four experiments are defined:

A **:** upwind scheme for momentum and salinity

B **:** TVD scheme for momentum, upwind for salinity

C **:** upwind scheme for momentum, TVD for salinity (default schemes of the program)

D **:** TVD scheme for momentum and salinity

A series of figures is produced showing the state at the end of the simulation for the four experiments: surface distributions of current and salinity (Figure 23.11), surface distributions of the vertical vorticity (Figure 23.12), current and salinity along a lateral transect parallel to the X-axis and through the axis of the cylinder (Figure 23.13).

In analogy with Tartinville et al. (1998) the volume-integrated kinetic energy, available potential energy and enstrophy are defined by

$$E_{kin} = \frac{1}{2}\rho_0 \int_{V(t)} (u^2 + v^2)\, dV \tag{23.12}$$

$$\begin{aligned} E_{pot} &= \int_{V(t)} \rho g x_3 \, dV - \rho_0 \int_{V_0} g x_3 \, dV_0 \\ &= \frac{1}{2} g \rho_0 \int_{S(t)} \zeta^2 \, dS - \rho_0 \int_{V(t)} b x_3 \, dV \end{aligned} \tag{23.13}$$

$$E_{str} = \int_{V(t)} \Big(\frac{\partial v}{\partial x_1} - \frac{\partial u}{\partial x_2} \Big)^2 dV \tag{23.14}$$

where $V(t)$ is the volume of the basin, V_0 its initial value, $S(t)$ the surface, ζ the surface elevation and $b = -g(\rho - \rho_0)/\rho_0$ the buoyancy. A fourth quantity a1% is defined as the surface area bounded by the contour line where the salinity is 0.01 PSU less than the ambient value of 34.85 PSU. This is determined by the number of surface grid cells where the salinity is less than 34.839 PSU multiplied by the area of a surface grid cell. Time series of these four quantities are plotted in Figures 23.14.

The following output parameters are defined for this test case:

ekin Volume integrated kinetic energy (10^9J) as defined by (23.12).

epot Volume integrated available potential energy (10^9J) as defined by (23.13).

enstr Volume integrated enstrophy (m^3/s^2) as defined by (23.14).

a1pt Value of a1% ($10^8 m^2$).

salmin The minimum salinity value (PSU) inside the domain.

salmax The maximum salinity value (PSU) inside the domain.

sdev In analogy with the test case ***seich*** this parameter represents the relative difference between the volume averaged salinity and its initial value and is, defined by

$$\text{sdev} = 10^6(\langle S(t)\rangle - \langle S(0)\rangle)/\langle S(0)\rangle \tag{23.15}$$

where a $\langle\ \rangle$ represents an averaged value over the entire domain. This parameter is useful for testing the machine accuracy.

theta The value of the ratio E_{kin}/E_{pot} averaged over an inertial period, determined by applying an harmonic analysis for the last 3 days (4.7 inertial periods).

23.4.3 Results

The following conclusions are made:

- A four-lobed structure is obtained. This is clearly observed in Figures 23.11d and 23.12d for scheme ***D*** and in a much weaker form for the other experiments.

- In analogy with the experimental results of Griffiths & Linden (1981) four cyclonic vortex rings develop at the points where the unstable displacements are directed inwards. The vortices are separated by areas with a weaker anticyclonic vorticity. The phenomenon is again

most clearly observed for scheme ***D***. This shows the ability of the TVD scheme to simulate highly sheared density fronts.

- The main circulation pattern consists of an outward (inward) displacement of the central area above (below) the interface, upwelling inside and below the fresh water patch with a maximum at the edge of core region and downwelling motions a few km outside the front. Note also the different depths of the fresh water layer in the four experiments. In the case of schemes ***C*** and ***D*** the interface depth decreases from 10 to 5–6 m giving a much shallower surface layer compared to ***A*** and ***B***.

- During the first hours of the simulation the kinetic energy increases at the expense of potential energy representing the outward expansion of the core region. As soon as a quasi-geostrophic balance is achieved and the eddies start to grow, both E_{kin} and E_{pot} oscillate with the inertial period and opposite phases. This quasi-equilibrium state is most clearly attained for experiment ***D***, whereas E_{kin} and E_{pot} gradually increase in the case of experiments ***A*** and ***B***. Note also that the vorticity, measured by the parameter E_{str}, is stronger in experiments ***B*** and ***D*** which use the TVD scheme for the advection of momentum. On the other hand, the surface area of the patch increases more rapidly for schemes ***A*** and ***B***. This is due to the larger numerical diffusion produced by the upwind scheme for salinity.

- According to Tartinville *et al.* (1998) the form and growth of the eddies is related to the ratio Θ of the kinetic to the available potential energy (represented here by the output parameter theta). Firstly, the number of baroclinic eddies given by the wavenumber n scales as $n \sim \Theta^{-1/2}$. Simulations using the PPM advection scheme both for salinity and currents (James, 1996) yield a value of Θ of $\sim$0.5 and a 2-lobed instability. This is comparable to the value obtained with scheme ***D*** in which case, however, a 4-lobed instability is found. Secondly, the growth rate of the instability increases with $\Theta^{1/2}$. This is, at least qualitatively, in agreement with the present results, as can be seen by comparing the development of the eddies in Figures 23.11 and 23.12 for experiments ***A, C, B*** and ***D*** which corresponds to increasing values of Θ.

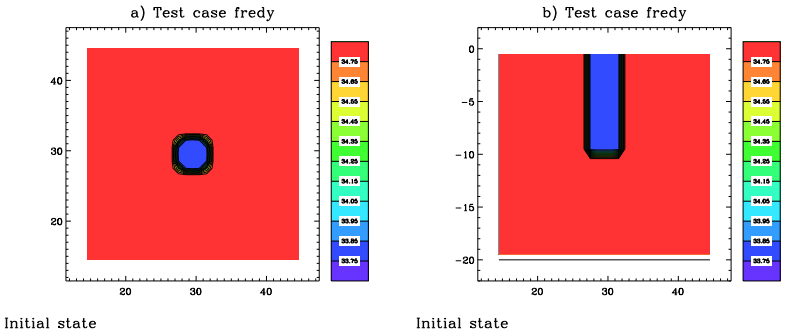

Figure 23.10: Initial salinity distribution for the ***fredy*** test case along the surface (a) and along a transect parallel to the X-axis and through the patch (b).

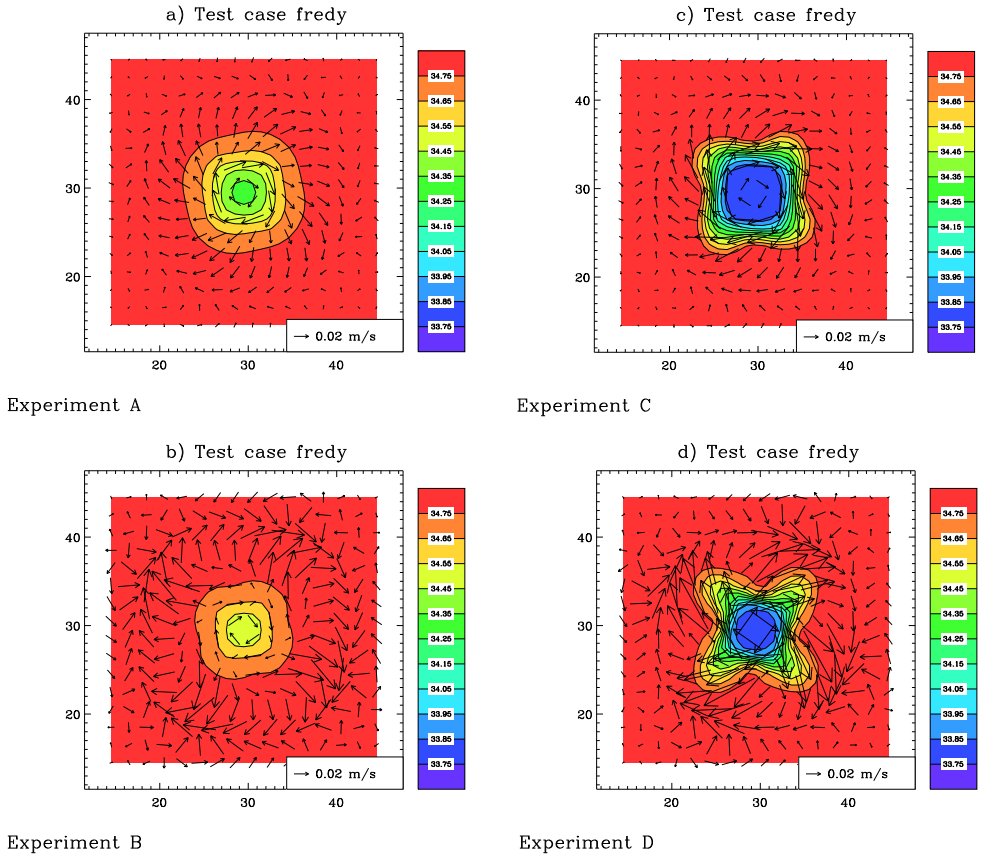

Figure 23.11: Test case ***fredy***. Surface current and salinity after 6 days for experiment ***A*** (a), ***B*** (b), ***C*** (c), ***D*** (d).

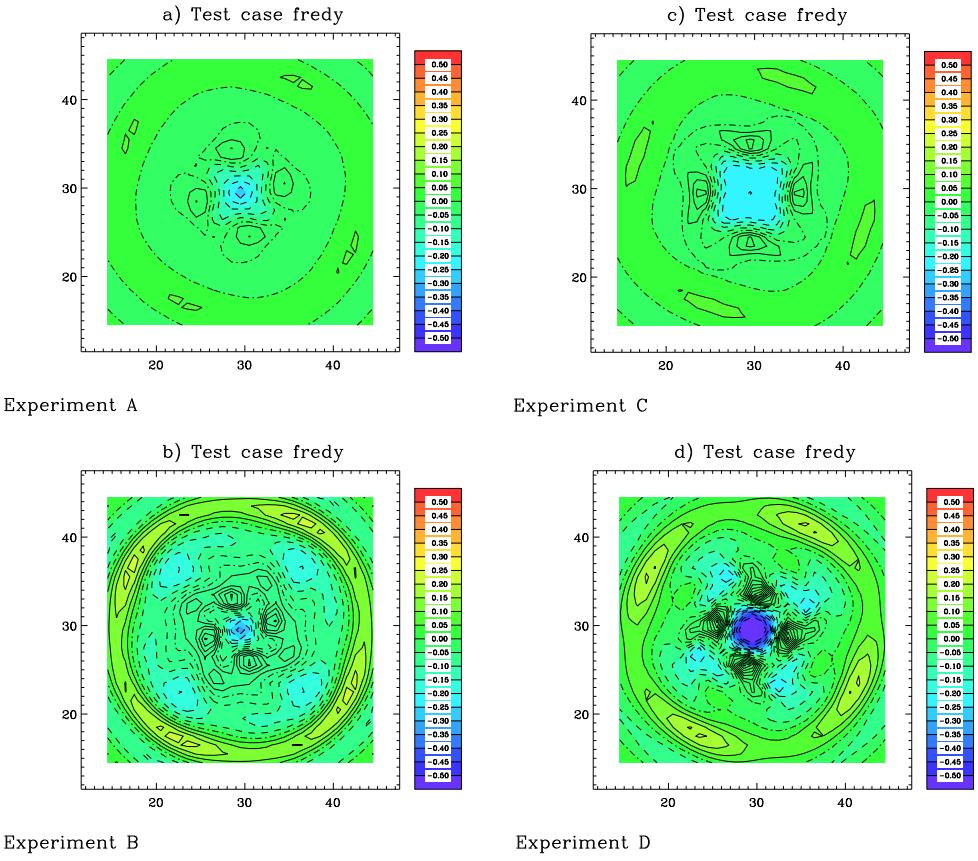

Figure 23.12: Test case ***fredy***. Surface vorticity normalised by the Coriolis frequency for experiment ***A*** (a), ***B*** (b), ***C*** (c), ***D*** (d).

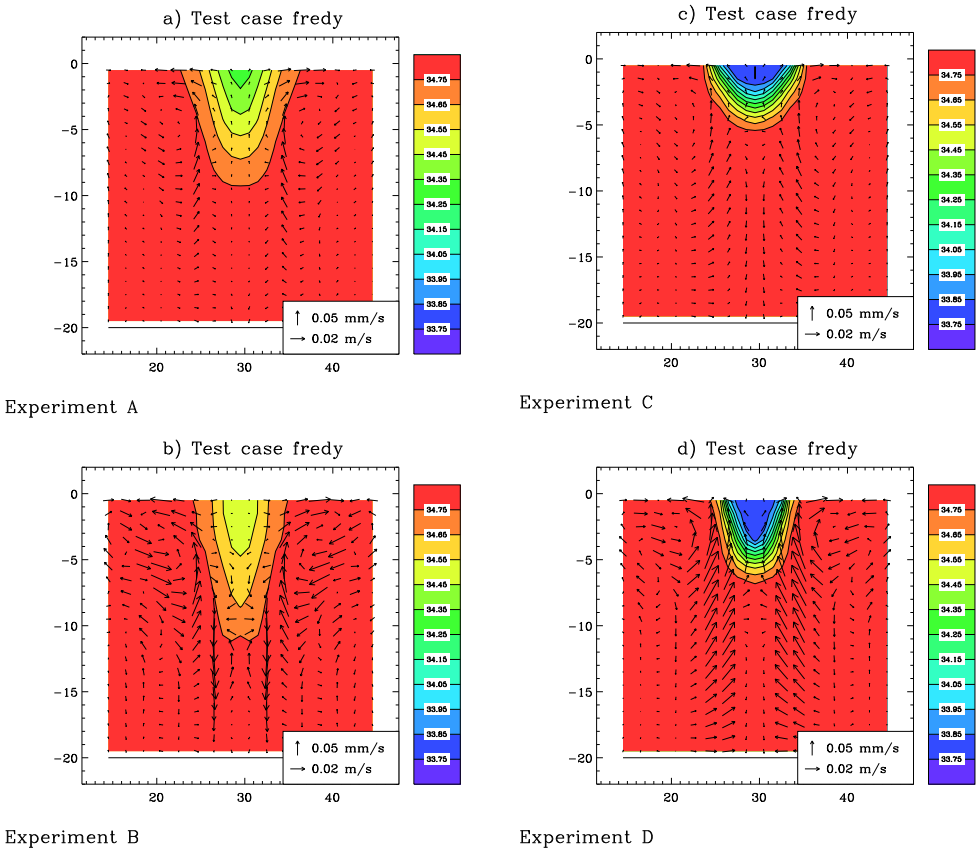

Figure 23.13: Test case ***fredy***. Current and salinity along a transect parallel to the X-axis and through the centre of the patch after 6 days for experiment ***A*** (a), ***B*** (b), ***C*** (c), ***D*** (d).

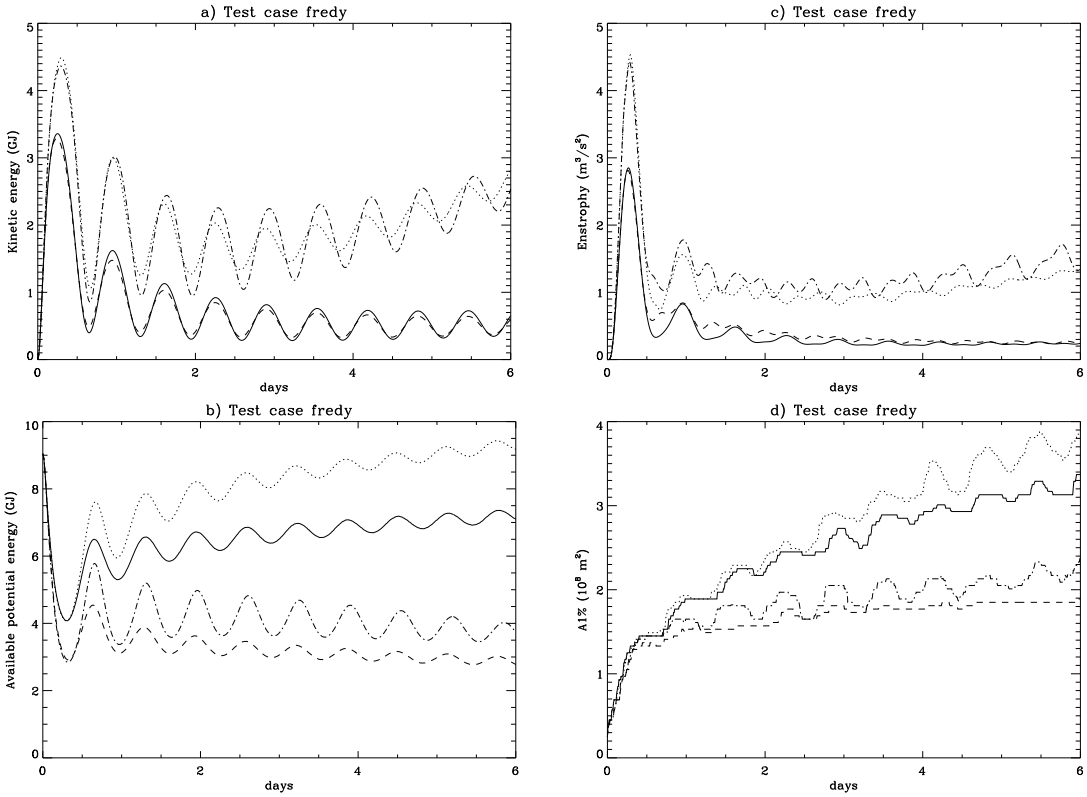

Figure 23.14: Test case ***fredy***. Time series of the kinetic energy E_{kin} in 10^9J (a), the available potential energy E_{pot} in 10^9J (b), the enstrophy E_{str} in m^3/s^2 (c) and the fresh water area A1% in units of $10^8 m^2$ (d) for experiment ***A*** (solid), ***B*** (dots), ***C*** (dashes), ***D*** (dash-dots).